15 August 2000

ELSEVIER

Optics Communications 182 (2000) 265–272

OPTICS COMMUNICATIONS

www.elsevier.com/locate/optcom

# Interference of converging spherical waves with application to the design of compact disks

Charles M.J. Mecca [a], Yajun Li [b], Emil Wolf [c,*]

[a] *WEA Manufacturing, Inc., 1400 East Lackawanna Avenue, Olyphant, PA 18448, USA*
[b] *527 Race Place, Oakdale, NY 11769, USA*
[c] *Department of Physics and Astronomy and Rochester Theory Center for Optical Science and Engineering, University of Rochester, Rochester, NY 14627, USA*

Received 8 May 2000; accepted 26 May 2000

**Abstract**

Two-point-source model is proposed to simulate the reflection of light from the data surface of a compact disk (CD). The returning field is modeled as arising from the interference of two converging spherical waves. The resulting field in the focal region exhibits maximum extinction (destructive interference) of light when the pit depth is optimized. For systems of small transverse magnification, the optimum pit depth is found to be one-half wavelength rather than a quarter wavelength as is customary assumed by the usual plane wave model. © 2000 Elsevier Science B.V. All rights reserved.

*Keywords:* Interference of converging waves; Compact disk; Data surface; Information pit; Transverse magnification; Order of interference; Focused fields

## 1. Introduction

The wave incident on a compact disk (CD) is focused on its data surface, on which numerous binary data are recorded in pits that are impressed along the CD surface and are covered with a very thin metal layer to ensure high reflection. A laser beam, focused by an objective lens, is used to read the data. It was claimed in several publications [1–3], based on elementary properties of interference between the incident and a reflected waves, that the maximum extinction of the returned light is obtained when the light reflected by a pit is in antiphase with the light reflected by the surrounding land, namely, when the pit depth is a quarter-wavelength. This criterion has been applied to CD manufacturing for many years. However, recent findings reveal that the quarter wavelength criterion may not predict optimum result under all circumstances [4].

To simulate the waves reflected from the CD data surface, we propose a two-point-source model. More specifically, two spherical (not plane) waves return from the disk and travel to the objective lens. One spherical wave is due to the reflection of the read-out beam from the pit, the other due to reflection from the surrounding land. The returning field then results from the superposition of two spherical waves, which first diverge from the disk and are then focused by the objective lens onto the photodetector. Conse-

* Corresponding author. Tel.: +1-716-275-4397; fax: +1-716-473-0687; e-mail: ewlupus@pas.rochester.edu


PII: S0030-4018(00)00772-0

quently, one is dealing with interference of two converging spherical waves with slightly different foci, slightly different focal lengths and slightly different cone angles rather than with interference of two plane waves. The focal regions of the two converging spherical waves are overlapping. In the common region, interference of the two focused spherical waves takes place.

In the present paper, we provide a model describing the interaction of two converging spherical waves in the focal region. This model is next applied to investigate how the binary data recorded on the CD

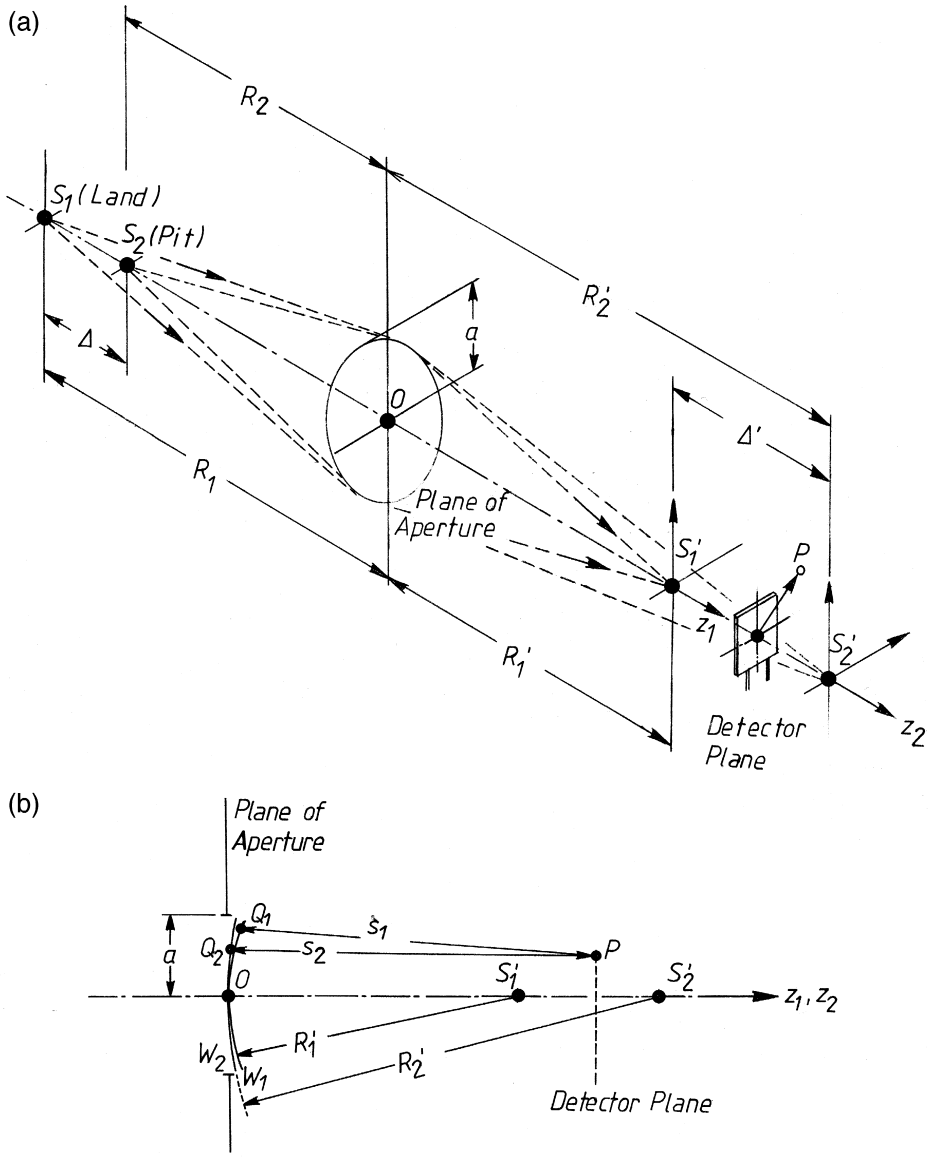


Fig. 1. The two-point-source model of light interaction with a CD: two monochromatic point sources $S_1$ and $S_2$, generating light of the same wavelength $\lambda$, are located on the axis of the objective lens. The point source $S_1$ is associated with reflection of the light from the land. The point source $S_2$ is associated with the reflection of the light from the pit. $\Delta$ denotes the pit depth. (a) Notation; (b) two wavefronts $W_1$ and $W_2$ of radii $R_1'$ and $R_2'$ are centered on the points $S_1'$ and $S_2'$ respectively and pass through the center $O$ of a circular aperture of radius $a$.

surface are transferred into a series of light pulses. We then calculate the optimum pit depth for which destructive interference leads to a maximum extinction of the light in the focal region.

## 2. Imaging of two point sources

Consider two point sources $S_1$ and $S_2$ of light of the same wavelength $\lambda$ are placed close to each other on the axis of a thin lens of focal length $f$ which fills an aperture of radius $a$ as shown in Fig. 1. Let

$$\Delta = R_1 - R_2 \tag{1}$$

be the separation of points $S_1$ and $S_2$, with $R_1$ and $R_2$ denoting the radii of curvature of the two spherical wavefronts immediately behind the thin lens. On the other side of the lens, two spherical wavefronts emerge, converging to points $S_1'$ and $S_2'$. We denote their radii of curvature by $R_1'$ and $R_2'$, respectively. For the point source $S_1$, the radii of curvature $R_1$ and $R_1'$ satisfy the lens relation

$$\frac{1}{R_1} + \frac{1}{R_1'} = \frac{1}{f}, \tag{2}$$

and for the point source $S_2$, the radii of curvature $R_2$ and $R_2'$ satisfy a similar relation

$$\frac{1}{R_2} + \frac{1}{R_2'} = \frac{1}{f}. \tag{3}$$

The separation of the image points $S_1'$ and $S_2'$ is given by (see Fig. 1(a))

$$\Delta' = R_1' - R_2' = -M_T^2 \times \Delta, \tag{4}$$

where $M_T$ is the transverse magnification of the system. Here we have assumed that the two spherical wave systems have the same transverse magnification.

## 3. Diffraction integrals

As we have indicated, we consider two spherical waves, say $V_1^{(i)}$ and $V_2^{(i)}$, generated by the two point sources $S_1$ and $S_2$, emerging from the aperture. At typical points $Q_1$ and $Q_2$ on the wavefronts which pass through the center $O$ of the aperture, the field distributions can be expressed in the form

$$V_1^{(i)}(Q_1,t) = A\frac{e^{-ikR_1'}}{R_1'}e^{-i\omega t}, \tag{5a}$$

$$V_2^{(i)}(Q_2,t) = A\frac{e^{-i(kR_2'+\theta_0)}}{R_2'}e^{-i\omega t}, \tag{5b}$$

where $A$ is a constant amplitude, $t$ denotes the time and

$$\theta_0 = k\Delta \tag{6}$$

is the phase shift introduced by the spatial separation $\Delta$ of the two point sources $S_1$ and $S_2$.

According to the Huygens–Fresnel principle (Ref. [5], Section 8.2), the diffracted fields at a point $P$ of the detector plane (see Fig. 1(b)) are given by the expressions (with time-periodic factor $\exp(-i\omega t)$ omitted)

$$U_1(P) = -\frac{i}{\lambda}\frac{Ae^{-ikR_1'}}{R_1'}\iint_{W_1}\frac{e^{iks_1}}{s_1}dS, \tag{7a}$$

and

$$U_2(P) = -\frac{i}{\lambda}\frac{Ae^{-i(kR_2'+\theta_0)}}{R_2'}\iint_{W_2}\frac{e^{iks_2}}{s_2}dS, \tag{7b}$$

where $s_1$ and $s_2$ denote the distances $Q_1P$ and $Q_2P$ and the integrals extend over the wavefronts $W_1$ and $W_2$ filling the aperture.

Let $(z_1,r_1,\psi_1)$ and $(z_2,r_2,\psi_2)$ be the two sets of cylindrical coordinates of the point $P$ in the focal regions of the two converging spherical waves originating from the point sources $S_1$ and $S_2$. The origins of the two coordinate systems are at $S_1'$ and $S_2'$, i.e., at the image points of the point sources $S_1$ and $S_2$. The $z$-coordinates of the two focusing systems have a separation $\Delta'$,

$$z_1 = z_2 + \Delta', \tag{8}$$

along the common direction $OS_1'$and $OS_2'$ (see Fig. 1(a)). The radial distances from the $z$-axes are

$$r_1 = r_2 = r \tag{9a}$$

and the azimuthal angles are also equal, i.e.,

$$\psi_1 = \psi_2 = \psi. \tag{9b}$$

It is convenient to introduce the Lommel parameters $(u_1,v_1)$ and $(u_2,v_2)$ which, together with the angle $\psi$, specify the position of the field point $P$:

$$u_1 = \left(\frac{a}{R_1'}\right)^2 kz_1, \tag{10a}$$

$$v_1 = \left(\frac{a}{R_1'}\right) kr_1; \tag{10b}$$

$$u_2 = \left(\frac{a}{R_2'}\right)^2 kz_2, \tag{11a}$$

$$v_2 = \left(\frac{a}{R_2'}\right) kr_2. \tag{11b}$$

Because the fields are rotationally symmetric about the $z$-axis, the diffracted fields are independent of the azimuthal angle $\psi$.

The photodetector which changes the intensity variations of the light into an electrical signal, is assumed to be placed at a point $z_1 = z_0$ in the focal regions of the two converging spherical waves. We then obtained from Eqs. (10) and (11) the following expressions for the Lommel parameters in the detector plane:

$$u_1 = \left(\frac{a}{R_1'}\right)^2 kz_0, \tag{12a}$$

$$v_1 = \left(\frac{a}{R_1'}\right) kr_1; \tag{12b}$$

$$u_2 = \left(\frac{a}{R_2'}\right)^2 k(\Delta' + z_0), \tag{13a}$$

$$v_2 = \left(\frac{a}{R_2'}\right) kr_2 = \left(\frac{R_1'}{R_2'}\right) v_1. \tag{13b}$$

Assuming, as is usually the case, that the focusing system of focal length $f$ has a high numerical aperture, the field in the region of the geometrical focus may be expressed in the form (Ref. [5], Section 8.8)

$$U(P) = -\frac{2\pi i a^2 A}{\lambda f^2} e^{i\left(\frac{f}{a}\right)^2 u} \int_0^1 J_0(v\rho)\, e^{-\frac{1}{2} i u \rho^2} \rho\, d\rho, \tag{14}$$

We now apply Eq. (14) to the two converging spherical waves discussed in Section 2.

On substituting $u = u_1$, $v = v_1$ and $f = R_1'$ into Eq. (13), we obtain for the diffracted field of the first converging spherical wave the expression

$$U_1(P) = -\frac{2\pi i a^2 A}{\lambda (R_1')^2} e^{i\left(\frac{R_1'}{a}\right)^2 u_1} \times \int_0^1 J_0(v_1\rho)\, e^{-\frac{1}{2} i u_1 \rho^2} \rho\, d\rho. \tag{15}$$

Similarly, on substituting $u = u_2$, $v = v_2$ and $f = R_2'$ into Eq. (13), we obtain the following expression of the diffracted field for the second converging spherical wave:

$$U_2(P) = -\frac{2\pi i a^2 A}{\lambda (R_2')^2} e^{i\left[\left(\frac{R_2'}{a}\right)^2 u_2 - \theta_0\right]} \times \int_0^1 J_0(v_2\rho)\, e^{-\frac{1}{2} i u_2 \rho^2} \rho\, d\rho. \tag{16}$$

The subscripts 1 and 2 affixed to the symbol $U(P)$ for the diffracted fields indicate that they originated from the point sources $S_1$ and $S_2$, respectively.

The field distribution in the focal region arising from the superposition of the two fields given by Eqs. (15) and (16) can be expressed as

$$\begin{aligned} U(P) &= U_1(P) + U_2(P) \\ &= -\frac{2\pi i a^2}{\lambda (R_1')^2} \left\{ e^{i\left(\frac{R_1'}{a}\right)^2 u_1} \times \int_0^1 J_0(v_1\rho)\, e^{-\frac{1}{2} i u_1 \rho^2} \rho\, d\rho \right. \\ &\quad \left. + e^{i\left[\left(\frac{R_2'}{a}\right)^2 u_2 - \theta_0\right]} \left(\frac{R_1'}{R_2'}\right)^2 \times \int_0^1 J_0(v_2\rho)\, e^{-\frac{1}{2} i u_2 \rho^2} \rho\, d\rho \right\}. \end{aligned} \tag{17}$$

According to Eq. (17), the intensity distribution $I(P) = |U(P)|^2$ in the focal region is, therefore,

$$\begin{aligned} I(P) = \left| 2 \left\{ \sqrt{I_{02}}\, e^{i\left(\frac{R_2'}{a}\right)^2 u_1} \int_0^1 J_0(v_1\rho)\, e^{-\frac{1}{2} i u_1 \rho^2} \rho\, d\rho \right.\right. \\ \left. + \sqrt{I_{02}}\, e^{i\left[\left(\frac{R_2'}{a}\right)^2 u_2 - \theta_0\right]} \times \int_0^1 J_0(v_2\rho)\, e^{-\frac{1}{2} i u_2 \rho^2} \rho\, d\rho \right\} \Bigg|^2, \end{aligned} \tag{18}$$

where

$$I_{01} = \left( \frac{\pi a^2 |A|}{\lambda (R_1')^2} \right)^2 \quad \text{and} \quad I_{02} = \left( \frac{\pi a^2 |A|}{\lambda (R_2')^2} \right)^2 \tag{19}$$

are constants.

## 4. The validity of Eq. (17) in the overlapping focal region

Eq. (17) is valid under the condition that the focal regions of two converging spherical waves overlap. Let us examine this situation.

The three-dimensional intensity distribution near the focus can be represented by isophotes, namely by contour lines of equal intensity (see Fig. 2 or Fig. 8.41 of Ref. [5]). Important for our consideration is the tubular structure in the bright central portion of the figure, which indicates the focal depth. The focal depths of the focused fields originated from the point sources $S_1$ and $S_2$ are of the order of (Ref. [5], see Eq. (27) in Section 8.8)

$$|\Delta z_1| = \frac{\lambda}{2} \left( \frac{R_1'}{a} \right)^2 \tag{20a}$$

and

$$|\Delta z_2| = \frac{\lambda}{2} \left( \frac{R_2'}{a} \right)^2 \tag{20b}$$

Hence Eq. (17) will be a good approximation provided that

$$|\Delta'| \lesssim |\Delta z_1| \tag{21a}$$

and

$$|\Delta'| \lesssim |\Delta z_2| \tag{21b}$$

On substituting from Eqs. (4), (20a) and (20b) into Eqs. (21a) and (21b), we obtain the following estimates for the range of validity of our theory:

$$M_T^2 \times \Delta \lesssim \frac{\lambda}{2} \left( \frac{R_1'}{a} \right)^2 \tag{22a}$$

and

$$M_T^2 \times \Delta \lesssim \frac{\lambda}{2} \left( \frac{R_2'}{a} \right)^2. \tag{22b}$$

With the choice $\Delta = \lambda/2$ and $M_T \approx (R_1'/R_1) \approx (R_2'/R_2)$, Eqs. (22a) and (22b) become

$$a \lesssim R_1 \tag{23a}$$

and

$$a \lesssim R_2 \tag{23b}$$

The numerical aperture of commonly used objective lens lies in the range between about 0.43 to 0.5, i.e., $R_1$ and $R_2$ are in the range between $1.73a$ and $2.10a$. Hence, the inequalities in Eqs. (23a) and (23b) are satisfied. We may, therefore, conclude that the focal regions of two converging spherical waves overlap and Eq. (17) correctly describes the combined effects of the two waves in the overlapping focal regions.

## 5. Interference effects in the focal region

To obtain a better insight into the structure of the region of superposition, we rewrite Eq. (18) in the form

$$I(P) = I_1(P) + I_2(P) + 2\sqrt{I_1(P) I_2(P)} \times \cos(\phi_1 - \phi_2), \tag{24}$$

where

$$I_1(P) = I_{01} \left| 2 \int_0^1 J_0(v_1 \rho) e^{-\frac{1}{2} i u_1 \rho^2} \rho d\rho \right|^2, \tag{25a}$$

and

$$I_2(P) = I_{02} \left| 2 \int_0^1 J_0(v_2 \rho) e^{-\frac{1}{2} i u_2 \rho^2} \rho d\rho \right|^2, \tag{25b}$$

are the intensity distributions in focal regions of the two converging spherical waves that represent the waves returning from the pit and from the surrounding land respectively on the data surface of a CD. After a long calculation, the phase factors $\phi_1$ and $\phi_2$ can be expressed in the form

$$\phi_1 = \left( \frac{R_1'}{a} \right)^2 u_1, \tag{26a}$$

$$\phi_2 = \left( \frac{R_2'}{a} \right)^2 u_2 - \theta_0. \tag{26b}$$

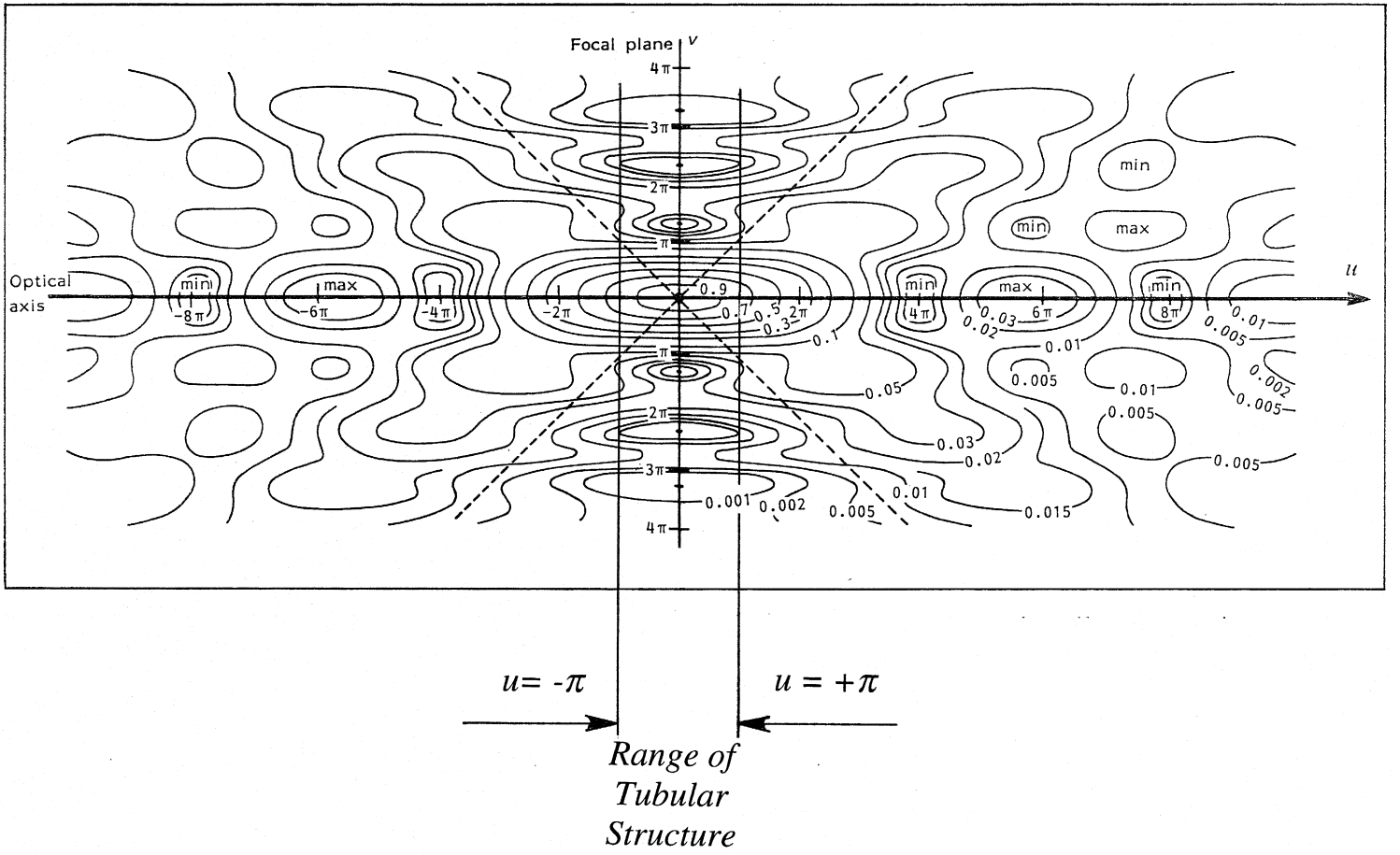


Fig. 2. Isophotes (lines of equal intensity) in the focal region. The tabular structure of the central portion should be noted [adapted from E.H. Linfoot and E. Wolf, Proc. Phys. Soc. B, 69 (1956) 823].

where $\theta_0$, given by Eq. (6), represents the phase shift between the two returned waves. Let us suppose that the photodetector is located at the distance

$$z_0 = -\Delta'/2 \tag{27}$$

from the point $S'_1$. It then follows Eqs. (12a) and (13a) that

$$u_1 = -k\left(\frac{a}{R'_1}\right)^2 \frac{\Delta'}{2} \tag{28a}$$

and

$$u_2 = k\left(\frac{a}{R'_2}\right)^2 \frac{\Delta'}{2}. \tag{28b}$$

On substituting Eqs. (28a) and (28b) into Eqs. (26a) and Eq. (26b), we obtain for the phase difference $\phi_1 - \phi_2$ the expression

$$\phi_1 - \phi_2 = \left(\frac{R'_1}{a}\right)^2 u_1 - \left(\frac{R'_2}{a}\right)^2 u_2 + \theta_0. \tag{29}$$

Next, on substituting from Eqs. (4), (6), (28a) and. (28b) into Eq. (29), we find that

$$\phi_1 - \phi_2 = -k\Delta' + k\Delta = k\Delta\left(1 + M_T^2\right). \tag{30}$$

When the laser spot on the disk surface scans over the pit, the phase difference $\phi_1 - \phi_2 = m\pi$, ($m = 1,3,5\ldots$). The intensity in the region of overlap is then a minimum and is given by the expression

$$I_{\min}(P) = I_1(P) + I_2(P) - 2\sqrt{I_1(P)\,I_2(P)}\,. \tag{31}$$

On the other hand, when the laser spot scans over the land, the phase difference $\phi_1 - \phi_2 = (m-1)\pi$, ($m = 1,3,5\ldots$). The intensity in the region of overlap is then a maximum and is given by the expression

$$I_{\max}(P) = I_1(P) + I_2(P) + 2\sqrt{I_1(P)\,I_2(P)}\,. \tag{32}$$

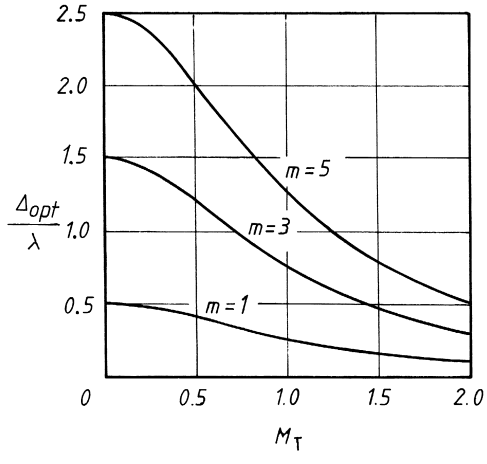


Fig. 3. Optimum pit depth $\Delta_{opt}$ as a function of the transverse magnification $M_T$ of the system, when $m = 1$, 3 and 5.

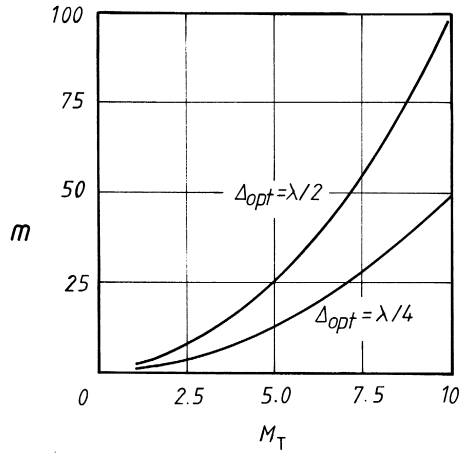


Fig. 4. The order of interference $m$ as a function of the transverse magnification $M_T$ of the system, when the optimum pit depth $\Delta_{opt}$ has the values $\lambda/2$ and $\lambda/4$.

The intensity distribution in the focal region in systems of large angular aperture is symmetrical about the focal plane (see Refs. [5] or [6]), viz.

$$I_1(-u_1, v_1) = I_1(u_1, v_1) \tag{33a}$$

and

$$I_2(-u_2, v_2) = I_2(u_2, v_2). \tag{33b}$$

If we ignore the slight difference between $R'_1$ and $R'_2$, we find immediately from Eqs. (28a) and (28b) that

$$u_1 \approx -u_2, \tag{34a}$$

and from Eqs. (12b) and (13b) that

$$v_1 \approx v_2. \tag{34b}$$

We can therefore conclude that

$$I_1(P) \approx I_2(P). \tag{34}$$

The maximum and minimum intensity distributions given by Eqs. (31) and (32) then reduce to

$$I_{\max}(P) \approx 4I_1(P) \tag{36a}$$

and

$$I_{\min}(P) \approx 0. \tag{36b}$$

The aim of pit-depth optimization is to bring the contrast, $C$ say, of the photodetector output signal to a maximum, namely, to insure that

$$C \equiv \frac{I_{\max}(P) - I_{\min}(P)}{I_{\max}(P) + I_{\min}(P)} \simeq 1. \tag{37}$$

This happens when $I_{\min}(P) = 0$, i.e., when

$$\phi_1 - \phi_2 = m\pi, \ (m = 1,3,5,\ldots). \tag{38}$$

On substituting from Eq. (30) into Eq. (38), one readily obtains for the optimum depth, $\Delta_{opt}$ say, of the information pit on the CD data surface the expression

$$\Delta_{opt} = \frac{\lambda}{2}\frac{m}{1 + M_T^2}, \ (m = 1,3,5,\ldots). \tag{39}$$

Eq. (39) is the main result of our analysis. In Fig. 3 the optimum pit depth $\Delta_{opt}$ is plotted as function of the transverse magnification $M_T$ for the cases when $m = 1$, 3 and 5.

## 6. Discussion and conclusions

It is seen from Eq. (39) that the optimum depth $\Delta_{opt}$ of the information pit is a function of three parameters: the wavelength $\lambda$, the transverse magnification $M_T$ of the system and the order of interference $m$. For systems of low magnification, namely, $M_T \ll 1$, and for the lowest order, $(m = 1)$, Eq. (39) gives

$$\Delta_{opt} \simeq \frac{\lambda}{2}. \tag{40}$$

However, the optimum depth $\Delta_{opt}$ decreases rapidly when the system magnification $M_T$ increases. The relationship between $M_T$ and the order of interference $m$ is shown in Fig. 4 for the cases when $\Delta_{opt} = \lambda/2$ and $\Delta_{opt} = \lambda/4$.

Finally, we mention that in our analysis we ignored the refraction of the returned waves at the boundary of the plastic substrate of CD. We plan to take it into account in another publication.

We may conclude by saying that we have shown that the optimum pit depth is a function of three parameters: the wavelength $\lambda$, the magnification $M_T$ of the system and the order of interference $m$. For a system of low magnification and for $m = 1$, the optimum pit depth is $\lambda/2$. However, for systems of large magnification, the optimum depth may take other values, including the conventional value $\lambda/4$.

## Acknowledgements

Our research was supported by the WEA Manufacturing, Inc.

## References

[1] G. Bouwhuis, J. Braat, A. Huijser, J. Pasman, G. van Rosemalen, K. Schouhamer Immint, Principles of Optical Disc Systems, 1st edn., Adam Hilger Ltd., Bristol and Boston, 1985.
[2] K.C. Pohlmann, The Compact Disc, updated edn., A–R Editions, Madison, 1992.
[3] J.G. Dil, B.A.J. Jacobs, J. Opt. Soc. Am. 69 (1979) 950.
[4] US Patent 5,995,481, November 30, 1999.
[5] M. Born, E. Wolf, Principles of Optics, 7th edn., Cambridge University Press, Cambridge, 1999.
[6] E. Collett, E. Wolf, Opt. Lett. 5 (1980) 264.